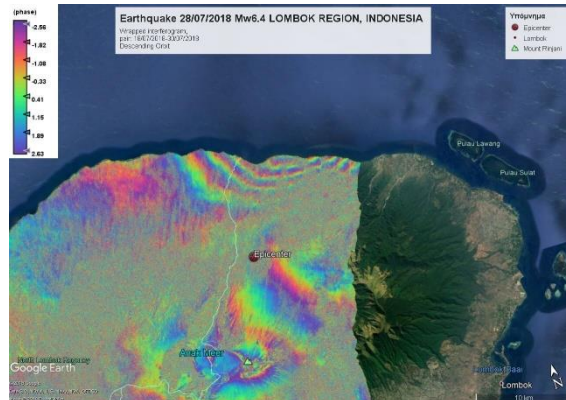


A preliminary
report on the 2018
Lombok region
Indonesia
earthquakes

August 9
2018

Athanassios Ganas,
Varvara Tsironi and
Sotirios Valkaniotis



A preliminary report on the 2018 Lombok region - Indonesia earthquakes

Athanassios Ganas¹ Varvara Tsironi¹ and Sotirios Valkaniotis²

¹ National Observatory of Athens, Institute of Geodynamics, 11810 Athens, Greece
aganas@noa.gr barbara.tsir@gmail.com

² 9 Koronidos Str., 42131 Trikala, Greece valkaniotis@yahoo.com

Abstract

Indonesia is considered as among the most active tectonic areas in the Asia – Pacific region. The July 28 2018, 22:47:37 UTC earthquake (M6.4, EMSC – followed by a M5.4 aftershock on 23:06 UTC) occurred on thrust fault which is part of the Flores fault zone of eastern Indonesia. A second, stronger event (M6.9, EMSC) occurred on August 5, 2018 11:46 UTC possibly on an adjacent segment of the fault zone towards the west (followed by a large aftershock occurred on August 9th, 2018 M5.9, EMSC). The earthquakes affected the island of Lombok in eastern Indonesia. Notably, a deep M6.0 earthquake had occurred several hundred kilometres to the east at 17:07 UTC on the day of the 1st event.

Due to shallow depth of the earthquakes and considering their M6+ magnitude (USGS; EMSC) significant ground deformation is expected. We investigated the surface earthquake effects using the ESA Sentinel satellites. Regarding InSAR processing we used data from Copernicus Sentinel-1 satellite constellation and ESA's SNAP open source toolbox. Data were downloaded from the Sentinel Open Access Hub. The differential interferogram provides an estimation of the relative motion of the earth surface in the direction viewing of the satellite (LOS). We obtained a maximum LOS displacement of **+28 cm** (towards the satellite) due to the combined motions of both events. We note these are preliminary results, as we did not analyse the contribution of the 2nd, stronger event. A 21-km long seismic fault is inferred from the Sentinel-1 fringe pattern as activated during the first event. We also detected numerous earthquake-induced landslides in Sentinel-2 imagery acquired on August 6, 2018.

Date of report

This report was released to EMSC-CSEM on August 9, 2018, 13:25 pm Greek time.

1. Geology and Tectonic setting

Indonesia is periodically affected by severe volcano eruptions and earthquakes, which are geologically coupled to the convergence of the Australian tectonic plate beneath the Sunda Plate. Global Positioning System (GPS) measurements of surface deformation (Kulali et al., 2016) show that the convergence between the Australian Plate and Sunda Block in eastern Indonesia is partitioned between the Java megathrust and a continuous zone of back-arc thrusting extending 2000 km from east Java to north of Timor (Fig. 1). Deformation of the upper plate is accommodated by slip partitioning, involving back-thrusting and strike-slip faulting forming a pattern of crustal blocks, parallel to the orientation of the Java-Timor trenches (Kulali et al. 2016; 2017).

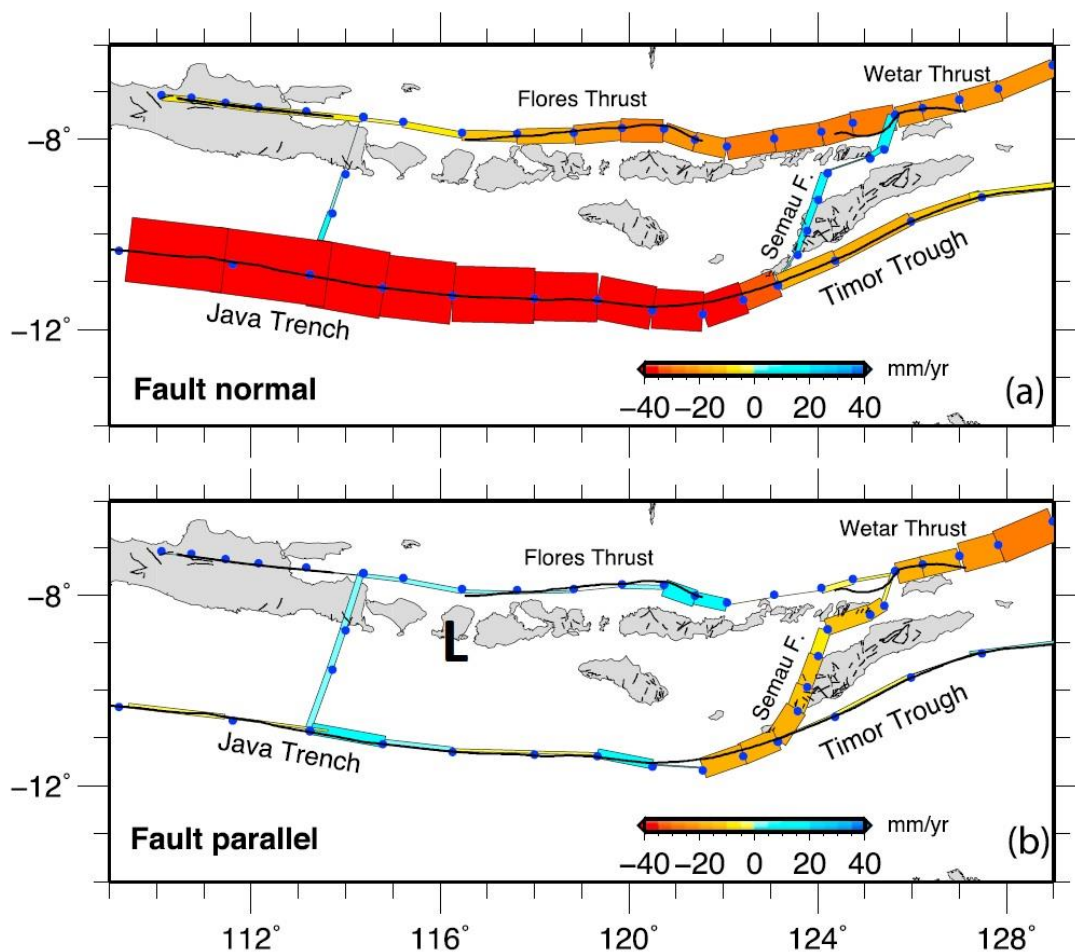


Figure 1. Maps of eastern Indonesia showing elastic block modelling results from GPS data: back-arc thrusting in the eastern Java trench area (incl. Lombok region; Flores thrust) is estimated between 1 and 2 cm/yr (Koulali et al., 2016). Fault slip rate components: (top) fault normal component (extension positive) and (b) fault parallel (right-lateral positive). The Lombok area is indicated with capital letter L.

In the bac-arc region, the prominent tectonic feature is the Kendeng – Flores thrust fault zone (Koulali et al., 2016, 2017; Fig. 1), a series of reverse fault segments spanning 2000

kilometres through the Indonesian archipelago. The fault zone accommodates a component of shortening between 1 and 2 cm/yr, in the direction normal to the Java megathrust (Fig. 1). The July-August 2018 shallow earthquakes occurred at the north Lombok island in eastern Indonesia near the Flores fault zone (see L in Fig. 1). The focal mechanisms of both events (solution summarized on the EMSC web site) indicate an almost east-west orientation of the ruptures and reverse kinematics. In particular, the July 28 2018, 22:47:37 UTC earthquake (M6.4, EMSC – followed by a M5.4 aftershock on 23:06 UTC) occurred onshore Lombok according to locations provided by EMSC and USGS. Eight days later, on 5 August 2018 (11:46 UTC) a stronger M6.9 event occurred in the same region. The 2nd earthquake heavily impacted buildings and infrastructures on northern Lombok¹ claiming 300 lives (as of August 9, 2018 date of this report). Notably, a deep M6.0 earthquake had occurred 700 kilometres to the ENE of the island at 17:07 UTC on 28 July 2018 or approx. five hours before the 1st event².

The rupture kinematics of both events was reverse as it was determined by the USGS moment tensor inversion (Table 1) while the hypocentre depths were shallow, at 6-31 km. The epicentre of the first event was located at 8.34°S, 116.48°E, according to EMSC, about 50 km to the NE of the capital Mataram. The epicentre of the 2nd event was determined by EMSC at 8.32° S, 116.46° E. Both epicentres are characterized by formal errors in location of about 4 km, however the actual errors are expected greater because of the lack of near-field seismic data. A large aftershock (M5.9) on August 9, 2018 05:25 UTC was located by EMSC at 8.42° S, 116.21° E.

Table 1. Nodal planes data from moment tensor inversion. Source: USGS.

Event	Mag	Strike-1	Dip-1	Rake-1	Strike-2	Dip-2	Rake-2
28/7/2018	6.4	276°	63°	96°	83°	28°	78°
5/8/2018	6.9	269°	62°	88	93°	28°	93°

The geology of Lombok island is mostly made of volcanic rocks (mainly tuffs, lahar, lavas and other volcanic deposits) due to the active Rinjani volcano (Fig. 2; https://en.wikipedia.org/wiki/Mount_Rinjani). The volcano rises to 3726 metres, making it the second highest volcano in Indonesia. Its last eruption was during August 2016 that generated an ash plume that rose to an altitude of 9.8 km (<http://volcano.si.edu/volcano.cfm?vn=264030>). The bedrock is made of carbonate rocks. It appears towards the south and southwest of the island (Fig. 2).

¹ <https://www.bbc.com/news/topics/c34zx89q9wkt/lombok-earthquakes>

² <https://www.emsc-csem.org/Earthquake/earthquake.php?id=700918>

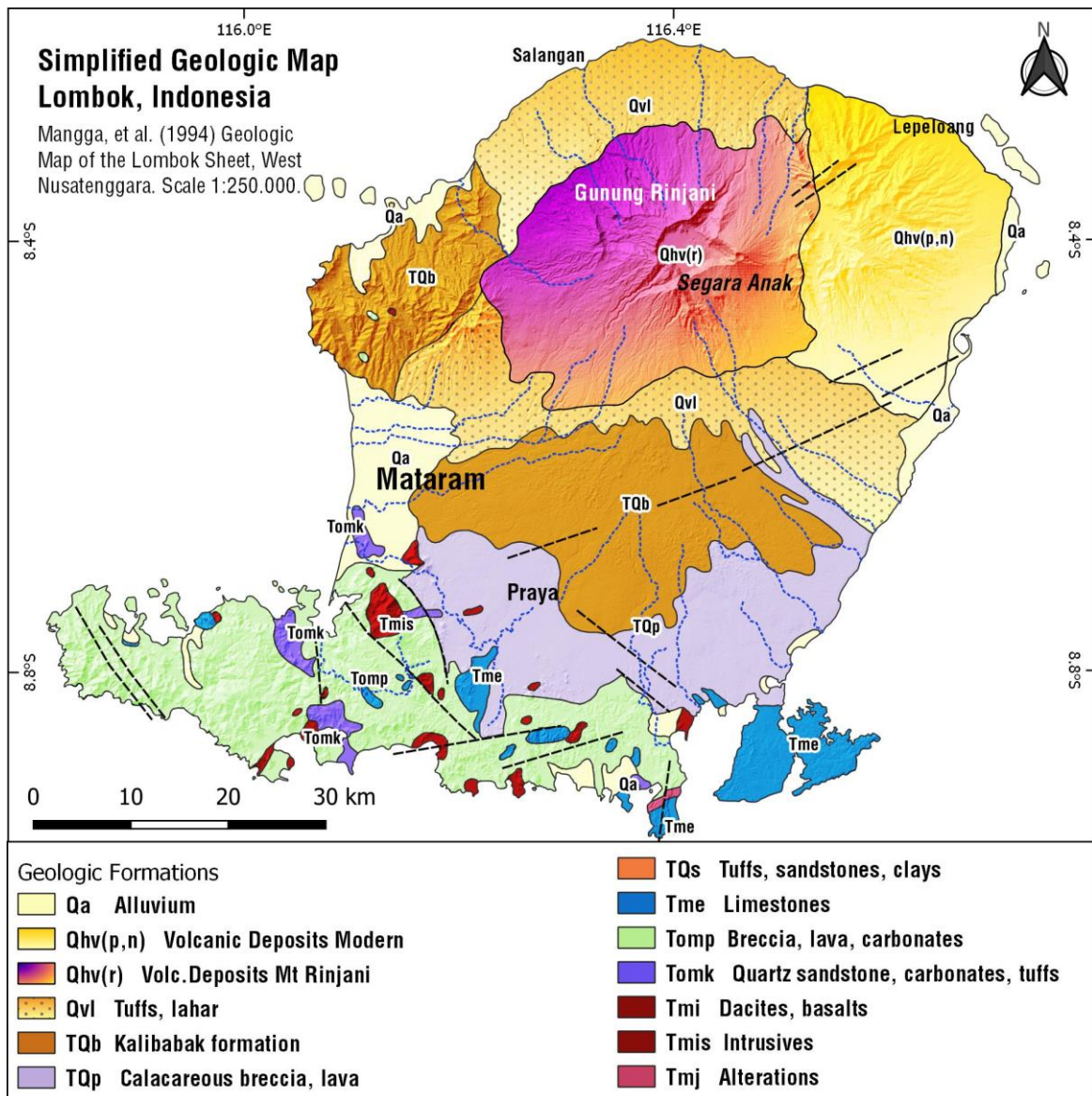


Figure 2. Simplified geological map of the Lombok island, Indonesia. Source: Mangga et al. (1994).

2. Satellite data

SAR interferometry (InSAR) is a geodetic technology based on RADAR sensors that can be used to support studying and modeling of terrain movements such as tectonic motions associated with faults and volcanic processes related to magma movements. The main advantages of InSAR is the synoptic view of wide areas (see Fig. 3 for the study area), and the periodic surveying that guarantees long-term monitoring and time series analysis. The availability of multiple signals permits the differentiation of tectonic vs. anthropogenic deformation, as well (e.g. Liu et al. 2016; Xu et al. 2017; Bovenga et al. 2018).

Here, we use Differential InSAR to capture the ground movements produced by the 28/07/2018 earthquake $M_w=6.4$ and the 05/08/2018 earthquake $M_w=6.9$ in the broader area of Lombok, Indonesia (Fig. 3). For InSAR processing, we used **ESA's SNAP** open source

software. We construct interferograms by combining topographic information with SAR images by the **Sentinel-1** (both 1A and 1B; C-band) satellite before and after the earthquakes. We used Sentinel-1 SLC images dated 18/07/2018 and 30/07/2018 for the first event and 24/07/2018 and 05/08/2018 for both events (see Fig. 4 for a timeline of acquisitions and events). The seismic events occurred on 28/07/2018 and 05/08/2018, so we had the opportunity to mostly map the co-seismic part of the ground deformation (the S1B August 5th image was acquired at 21:52 UTC or about 10 hours after the 2nd event). Details of the interferometric pairs for both interferograms which are constructed in this study are reported in Table 2. We also plan to process ascending orbit images when they are fully available so we can differentiate the deformation due to the 2nd event and possibly the deformation due to the large aftershock of August 9, 2018. The acquisition strategy of Sentinels is suited well to the needs of the tectonics community as it provides frequent images for mapping deformation due to earthquakes occurring closely in space and time (e.g. Ganas et al. 2018).

The interferograms were flattened and topographic phase compensated for based on a reference SRTM Digital Terrain Model (~90 m resolution). In order to reduce the effects of phase noise adaptive filtering (Goldstein & Werner, 1998) was applied, in addition to multilooking operation using a factor of 10:2 (azimuth : range) obtaining approximately a square pixel interferogram.

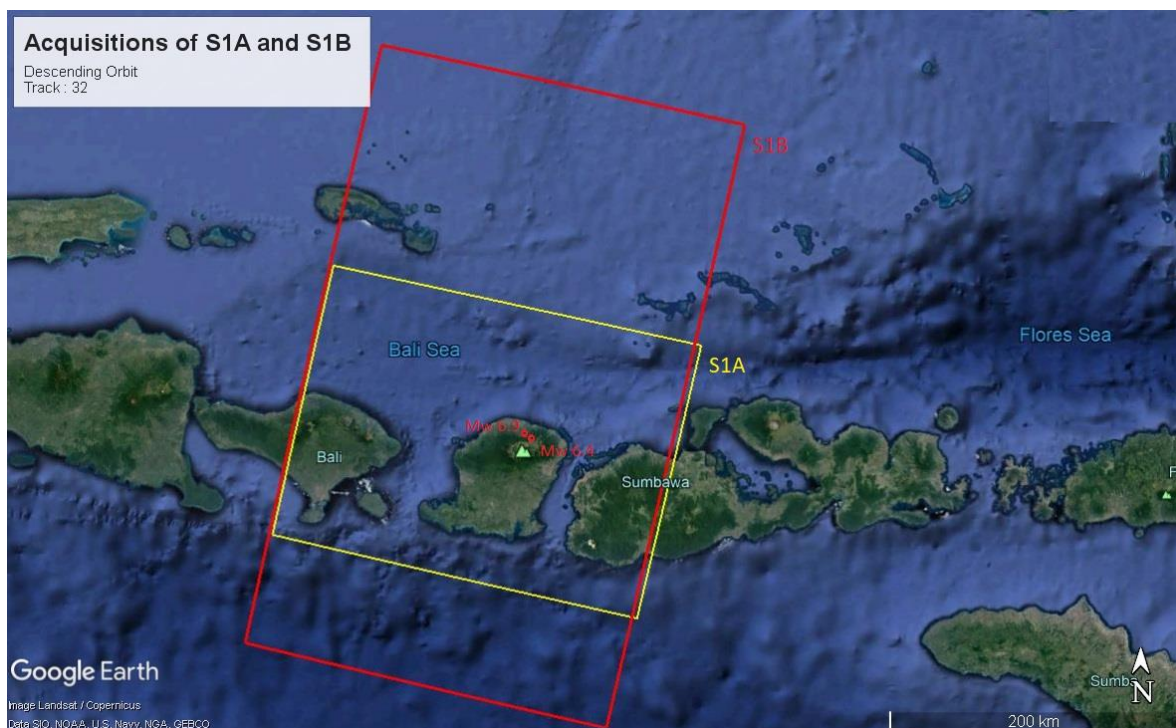


Figure 3. Google map showing the Sentinel frames (descending orbit) over the earthquake-struck region.

Table2. Characteristics of the interferometric pair used to study the 2018 Lombok earthquakes. See Fig. 4 for a timeline.

Orbit	Satellite	Track	Master	Slave	Bperp (m)	Incidence Angle (°)
Descending	S1A	32	2018-07-18 T21:53:00.671Z	2018-07-30 T21:53:01.272Z	-76.09	43.5
Descending	S1B	32	2018-07-24 T21:52:23.776Z	2018-08-05 T21:52:24.073Z	-117.69	43.4

The wrapped interferograms show the fringe pattern associated with the earthquakes, where each color cycle demonstrates a phase difference of $[-\pi \pi]$, interpreted as ground deformation equal to 2.8 cm in the LOS (*Line Of Sight*) direction to the satellite. The quality of the interferograms was good but we obtained noisy areas which are the result of low coherence. These areas have dense vegetation cover. The deformation was localized at the north part of the island, near to the $M_w=6.4$ and $M_w=6.9$ epicentres.

We obtained a preliminary, maximum LOS displacement of **+14 cm** from the interferogram of first event (Fig. 5; see five fringes of 28 mm motion each) and a preliminary, maximum LOS displacement of **+28 cm** (towards) [and a minimum LOS Displacement -8.4 cm (away)] from the interferogram which corresponds to both events (Fig. 6). Although the interpretation is preliminary we note that the sign reversal in the InSAR data (Fig. 6) may indicate that the activated fault during the 2nd event may actually outcrop near the NW coast of Lombok.

Due to the reverse-slip kinematics of the earthquakes (determined by seismology; Table 1) we infer that the motion towards the satellite indicates surface uplift (the fringe pattern also indicates motion increasing towards the coast; Fig. 5), therefore the mapped fringes indicate deformation of the *hangingwall* of the activated thrust faults. We note these are preliminary results as no ascending orbit data were processed.

The deformation field after the occurrence of the 2nd event (image pair 24/7/2018 – 5/8/2018) can be visualized by the larger number of sub-parallel fringes as compared to the fringe pattern of the 1st event (compare Fig. 5 vs. 6). The fringes also indicate ground deformation towards the satellite (i.e. surface uplift). This pattern implies that the 2nd event is affecting the coastal area to the west and northwest of the 1st event so as it is inferred that the 5/8/2018 rupture area comprises another segment to the west of the 28/7/2018 or it represents the western asperity of a large reverse fault beneath Lombok’s north coast.

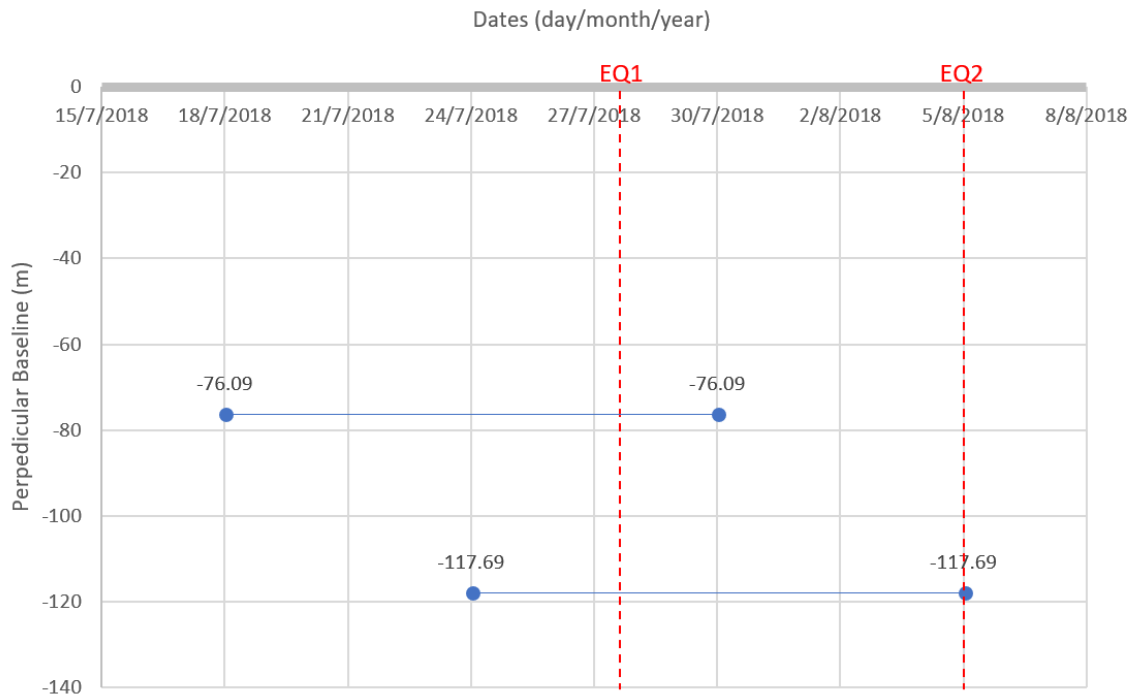


Figure 4. S1 Interferometric baselines from S1 descending track 32 (blue horizontal lines). Acquisition dates are plotted over the line ends. The vertical red dashed lines show the seismic events EQ1: 28/07/2018 earthquake $M_w=6.4$, EQ2: 05/08/2018 earthquake $M_w=6.9$.

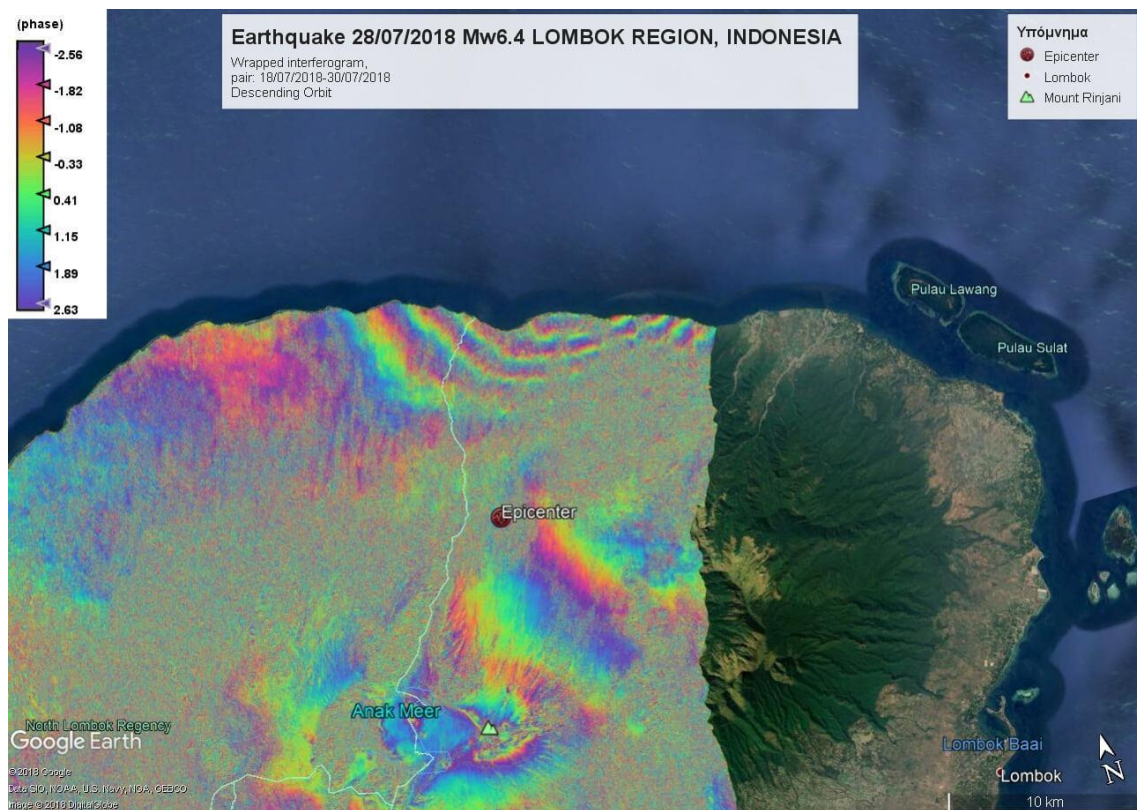


Figure 5. Sentinel 1A wrapped interferogram (descending orbit) showing LOS deformation onshore Lombok island, Indonesia due to the M6.4 28/7/2018 event. Five fringes are visible to the north of the EMSC epicentre.

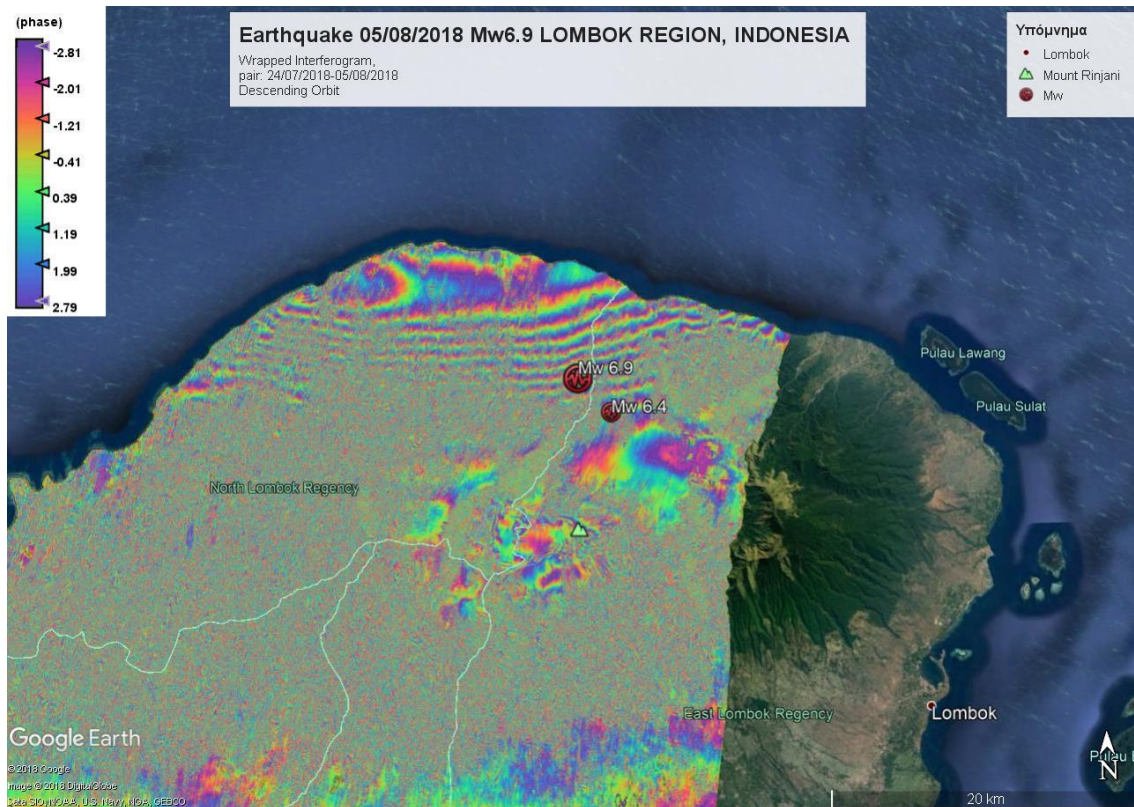


Figure 6. Sentinel 1B wrapped interferogram showing LOS deformation onshore Lombok island, Indonesia due to the 28/7/2018 & 5/8/2018 earthquakes. A sign reversal (from positive to negative LOS motion) is seen in the NW coastal area. Note the difference in scale bar at lower right w.r.t Fig. 5.

3. Fault modeling

A preliminary elastic modeling³ of the co-seismic displacements together with LOS displacements from SAR interferometry (Fig. 5) gives the following preliminary parameters for the fault that ruptured during the 1st event (Table 3). The modelled fringe pattern is almost similar for both dip-direction scenarios (north vs. south). Because of the onshore location of the epicentre a south-dipping, low-angle plane (25°) is favored. The depth to the top of the fault is 5 km, the depth to the fault bottom is 9.2 km. Half of the rupture is modelled offshore (Fig. 7).

Table 3. Lombok 28 July 2018 earthquake fault parameters. See Fig. 7 for plots.

Fault length	21 km
Fault width	10 km
Fault Dip angle	25° south
Azimuth	N87°E
Rake of slip vector	80°
Fault Slip	0.9 m
Centre of upper edge of the fault	116.58° E - 8.21° S

³ made with RINGCHN, Feigl and Dupre, 1999

The seismic moment from this geodetic model is 5.67×10^{18} N-m (the USGS seismic moment from radiated seismic waves⁴ is 5.639×10^{18} N-m or 1% less).

Our forward modeling shows that the reverse-slip rupture has an ENE-WSW orientation and the plane dips to the south. The rupture extent is estimated at 20-21 km. Moreover, to the east the rupture extent is ambiguous due to lack of data (end of satellite frame). It is possible that the 5 August event ($M_w=6.9$) possibly ruptured a western extension of about 25-30 km length.

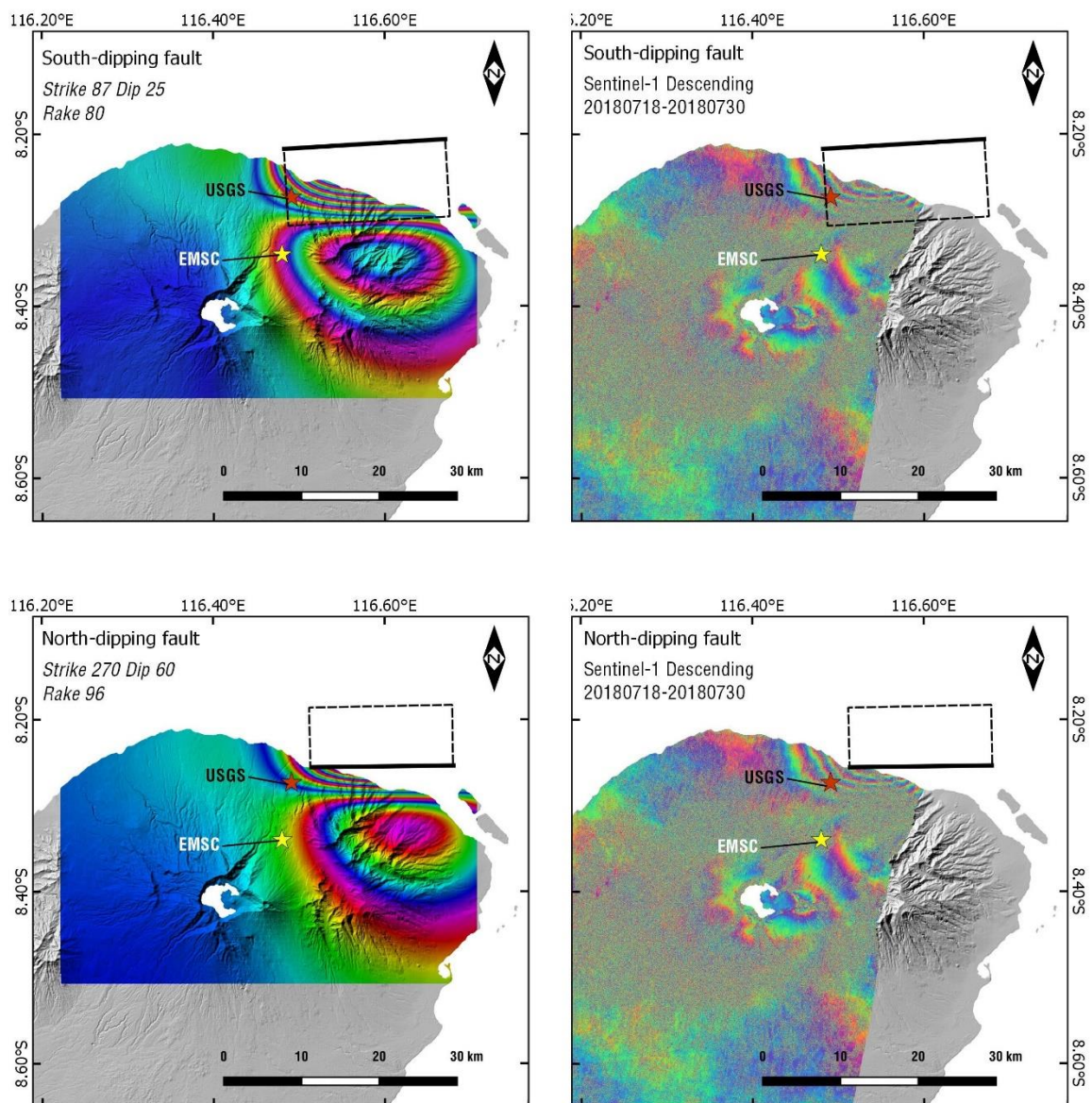


Figure 7. Preliminary fault models based on InSAR data (black rectangle indicates surface projection of seismic fault). Left) models Right) S1 interferograms. Upper row shows the south-dip (favoured) scenario, lower row the north-dip scenario, respectively.

⁴ <https://earthquake.usgs.gov/earthquakes/eventpage/us2000ggs#moment-tensor>

4. Geo-environmental Effects and surface ruptures

The August 5th $M_w=6.9$ earthquake caused widespread landslides at the northern part of Lombok island. Although field reports are limited at this time, Sentinel-2 satellite imagery from Copernicus, acquired few hours after the earthquake (2018-08-06 UTC 02:39; Fig. 8), reveals numerous landslides. Although the August 6th acquisition has cloud patches that mask parts of Mt Rinjani, thousands of estimated landslides are visible on the volcanic slopes of Mt Rinjani, mostly on western, northern and eastern slopes. Landslides on the low relief coastal areas are limited and are found mainly on the steep banks of rivers. The Sentinel-2 pixel resolution limits the analysis on landslides to those with dimensions larger than 10 m. Smaller landslides are probably widespread and numerous, and could be verified by field mapping reports, commercial very high resolution satellite imagery and UAVs (e.g. Valkaniotis et al. 2017).

The intensity of the shaking of the 2nd event possibly reached **0.4 g** according to the USGS shake map⁵ while the region seems heavily susceptible to landslides because of relatively-incoherent volcanic deposits and reduced strength of materials due to past, strong earthquakes. Accelerations up to 0.1 g may have occurred at distances up to 50 km from the epicentre.

A Sentinel-2 acquisition of August 1st 2018, permits a limited separation of landslides from the two main events. A larger percent of cloud cover on the August 1st image limits the analysis, but from a preliminary examination we conclude that landslides from the July 28th $M_w=6.4$ event are significantly fewer in number and are mostly limited on the eastern slopes and near the summit area of Mt Rinjani volcano. Thus, comparing Sentinel-2 images from July 12, August 1 and August 6, the majority of landslides occurred from the $M_w=6.9$ earthquake.

Due to the close timing of the August 6th satellite acquisition (14+ hours after) with the main $M_w=6.9$ event, Sentinel-2 has captured the magnitude of landslide and rockfall occurrence around the crater lake *Segara Anak*, at the summit of Mt Rinjani: high resolution imagery shows the dust cloud still present around the steep cliffs from the main shock and the first aftershocks⁶, along with recent landslide debris on the slopes and on the lake (Figure 9). An example of earthquake-induced landslides is shown in Fig. 10.

⁵ <https://earthquake.usgs.gov/earthquakes/eventpage/us1000g3ub#shakemap>

⁶ A $M_w=5.3$ occurred on 6/8/2018 00:28 UTC <https://www.emsc-csem.org/Earthquake/earthquake.php?id=704921>

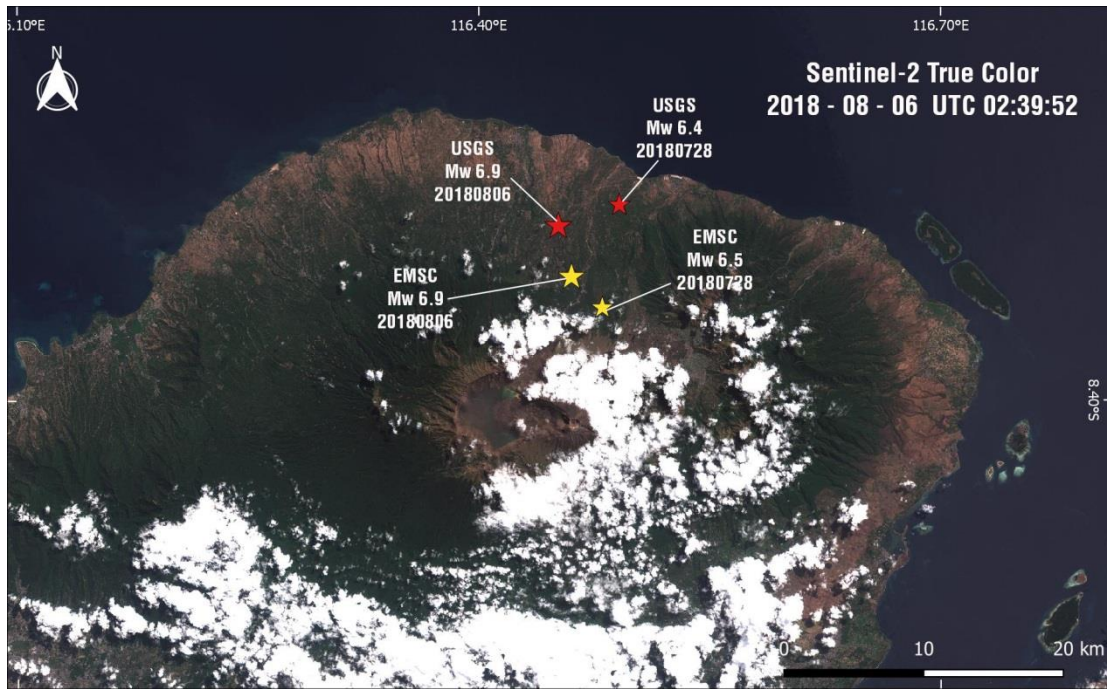


Figure 8. Sentinel-2 image of Lombok island, August 6th 2018, 02:39 UTC. Epicentres of the two main earthquakes (July 28th and August 5th) from USGS and EMSC shown as stars.

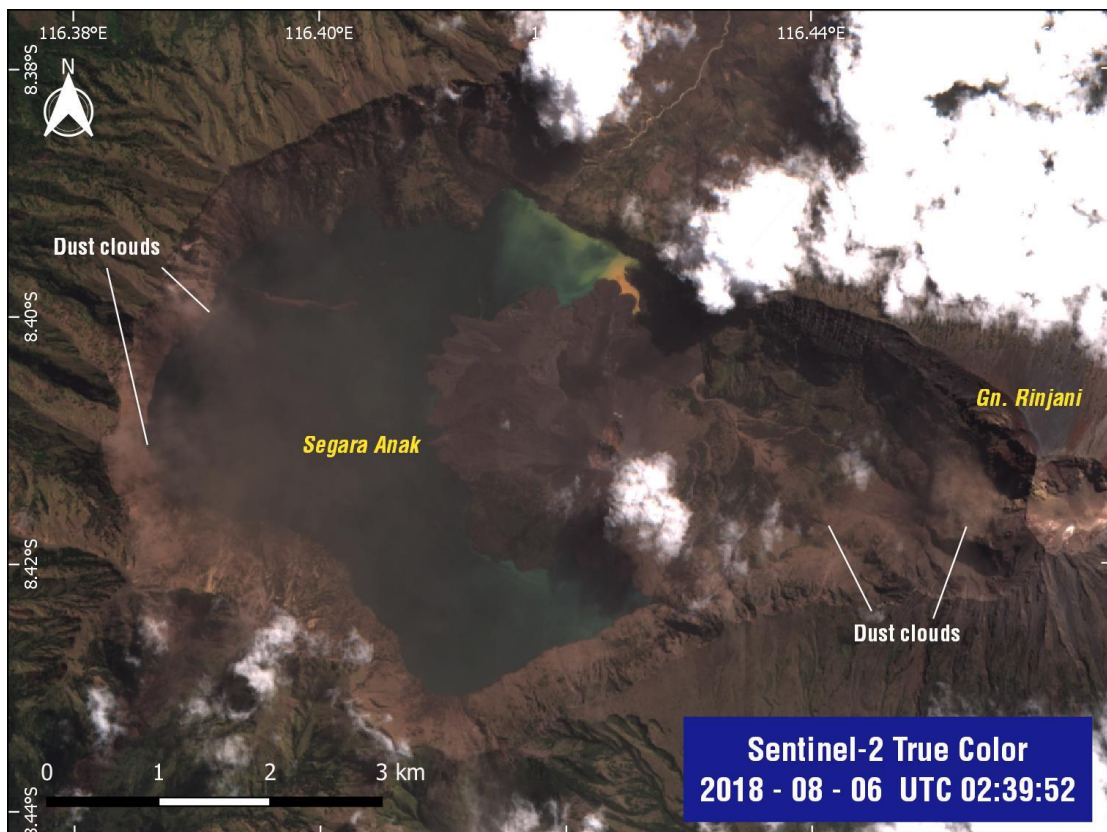


Figure 9. Sentinel-2 image showing widespread landslides, debris, dust clouds & sediment aftermath of the August 5th earthquake and aftershock activity. Zoom at Segara Anak lake at Mt Rinjani. Acquisition time is ~14 hrs after the $M_w=6.9$ event.



Figure 10. Examples of landslides from the August 5th $M_w=6.9$ earthquake, with comparison of pre- and post- earthquake Sentinel-2 true colour imagery (August 1st on the left, August 6th on the right). Location is at 116.300° E - 8.352° S.

5. Acknowledgments

We thank ESA and Copernicus for satellite (S1 & S2) acquisition imagery. We also thank Pierre Briole for comments.

6. References

Bovenga F., A. Ganas, A. Refice, A. Belmonte, R. Nutricato, D. O. Nitti, M. T. Chiaradia, S. Valkaniotis, S. Gkioni, C. Kosma, P. Manunta, E. Elizar, D. Darusman, and P. Bally, 2018. Investigating ground instability in Indonesia by using multi temporal SAR interferometry, *Geophysical Research Abstracts* Vol. 20, EGU2018-8488.

Feigl, Kurt L., Emmeline Dupre, 1999. *RNGCHN: a program to calculate displacement components from dislocations in an elastic half-space with applications for modeling geodetic measurements of crustal deformation*. *Computers & Geosciences*, 25, 695-704.

Ganas, A, Kourkouli, P, Briole, P, Moshou, A, Elias, P, Parcharidis, I, 2018. Coseismic Displacements from Moderate-Size Earthquakes Mapped by Sentinel-1 Differential Interferometry: The Case of February 2017 Gulpinar Earthquake Sequence (Biga Peninsula, Turkey). *Remote Sens.*, 10, 1089, <http://www.mdpi.com/2072-4292/10/7/1089>

Goldstein, R., Werner, C., 1998. *Radar interferogram filtering for geophysical applications*. *Geophys. Res. Lett.* 25, 4035–4038.

Koulali, A., S. Susilo, S. McClusky, I. Meilano, P. Cummins, P. Tregoning, G. Lister, J. Efendi, and M. A. Syafi'i, 2016. *Crustal strain partitioning and the associated earthquake hazard in*

the eastern Sunda-Banda Arc. Geophys. Res. Lett., 43, 1943–1949, doi:10.1002/2016GL067941.

Koulali, A., et al. 2017. The kinematics of crustal deformation in Java from GPS observations: Implications for fault slip partitioning, Earth and Planetary Science Letters, Volume 458, Pages 69-79, <https://doi.org/10.1016/j.epsl.2016.10.039> .

Liu, P.; Li, Q.; Li, Z.; Hoey, T.; Liu, G.; Wang, C.; Hu, Z.; Zhou, Z.; Singleton, A., 2016. Anatomy of Subsidence in Tianjin from Time Series InSAR. Remote Sens., 8, 266.

Mangga, S.A., et al. 1994. *Geological map of the Lombok sheet, west Nusatenggara*. Scale 1:250.000.

Valkaniotis S., A. Ganas, and G. Papathanassiou, 2017. Using a UAV for collecting information about a deep-seated landslide in the island of Lefkada following the 17 November 2015 strike-slip earthquake (M=6.5), Geophysical Research Abstracts Vol. 19, EGU2017-9376, 2017.

Xu, X., D. T. Sandwell, E. Tymofyeyeva, A. González-Ortega and X. Tong, 2017. Tectonic and Anthropogenic Deformation at the Cerro Prieto Geothermal Step-Over Revealed by Sentinel-1A InSAR. IEEE Transactions on Geoscience and Remote Sensing, vol. 55, no. 9, pp. 5284-5292, doi: 10.1109/TGRS.2017.2704593.

web sites (last accessed August 9, 2018)

<https://www.emsc-csem.org/Earthquake/earthquake.php?id=704824>

<https://www.emsc-csem.org/Earthquake/earthquake.php?id=701004>

<https://www.emsc-csem.org/Earthquake/earthquake.php?id=705531>

<https://earthquake.usgs.gov/earthquakes/eventpage/us1000g3ub#executive>

<https://earthquake.usgs.gov/earthquakes/eventpage/us2000ggbs#executive>

END of REPORT